The Effect of Trapped Gas on Foam Flow in a Model Porous Medium

Jones, Sian; Getrouw, N.; Vincent-Bonnieu, Sebastien

DOI
10.3997/2214-4609.201700338

Publication date
2017

Document Version
Final published version

Published in
IOR NORWAY 2017

Stavanger NORWAY
The National IOR Centre of Norway
EAGE

We B11

The Effect of Trapped Gas on Foam Flow in a Model Porous Medium

S.A. Jones (Technical University of Denmark & TU Delft), N. Getrouw (TU Delft) & S. Vincent-Bonnieu* (Shell Global Solutions Int. B.V. & TU Delft)

SUMMARY

Foams for enhanced oil recovery can increase sweep efficiency, as they decrease the gas relative permeability, mainly due to gas trapping. However, gas trapping mechanisms are poorly understood. Some studies have been performed during corefloods, but little work has been carried out to describe the bubble trapping behaviour at the pore scale.

Microfluidic experiments are a useful tool for studying the foam flow behavior at the pore scale. We have carried out foam flow tests in a model porous media glass micromodel. Image analysis of the foam flow allowed local velocities to be obtained. The quantity of trapped gas was measured both by considering the fraction of bubbles that were trapped (via velocity thresholding) and by measuring the area fraction containing immobile gas (via image analysis). A decrease in the trapped gas fraction was observed both for increasing total velocity and for increasing foam quality.

Calculations of the gas relative permeability were made with the Brooks Corey equation, using the measured trapped gas saturations. The results showed a decrease in gas relative permeabilities for increasing fractions of trapped gas. It is suggested that the shear thinning behaviour of foam could be coupled to the saturation of trapped gas.

Introduction

Gas trapping is an important mechanism that occurs during Water/Surfactant Alternating Gas (WAG/SAG) and foam injection processes. When gas is trapped in place, the overall gas mobility is reduced, which then reduces the relative permeability of the gas phase. (Falls *et al*., 1989; Kovscek *et al*., 1994; Kovscek and Bertin, 2003).

Although trapped gas is of great importance in the understanding of foam behaviour in a porous media, there are only a few experimental studies on this subject, probably due to the technical challenges involved in differentiating between stationary and moving gas within a rock core. Most studies have focused on injecting a foam, then once steady state flow has been obtained a tracer gas is injected with the foam. The quantity of trapped gas can then be determined either by using CT imaging to visualize the tracer (Nguyen *et al*., 2009; Kil *et al*., 2011) or by sampling the effluent to determine the concentration of tracer (Friedmann *et al*., 1991; Radke and Gillis, 1990; Tang and Kovscek, 2006). However, there are potential errors linked to these tracer measurement techniques due to the fact that the flow paths within the core can fluctuate with time. Any fluctuations can cause a false reading of the number of flowing paths that appear to be open and could thus cause an overestimation of the fraction of moving gas and an underestimation of the trapped gas fraction (Kil *et al*., 2011).

Even ignoring any potential underestimation, the quantity of gas trapped in a porous medium is still significant. Radke and Gillis (1990) found trapped gas fractions of between 70% and 100% for all their tests, with superficial velocities in the range of 0.5 to 4 m/day and foam qualities between 0.8 and 1.0 respectively. Friedman *et al*. (1991) also measured trapped gas fractions in the range 75% to 90% over a wide range of velocities (from 25 up to 150 m/day). In both these cases, the authors found only a small variation in the trapped gas with changing velocity, with Radke and Gillis (1990) observing a slight trend towards higher values of trapped gas with higher velocities.

In contrast, Tang and Kovscek (2006) found a significant decrease in trapped gas with increasing gas velocity (and a constant liquid velocity of 0.19 md^{-1}), with the trapped gas fraction dropped from 87% at a gas velocity, u_g, of 0.55 md^{-1} to 56% at 30.4 md^{-1}. They also showed a dependence of the trapped gas on foam quality, with drier foams giving lower values of trapped gas.

In order to investigate some of these issues further, we have carried out foam flow tests, with a focus on trapped gas, in a model porous medium etched in a 2D glass microfluidic chip. In a 2D geometry, the foam behaviour can be easily visualised and quantified, and the number of trapped bubbles can be determined at any single time. With this experimental setup it was possible to determine the dependency of the fraction of trapped gas on foam quality, linear velocity and location within the micromodel. In addition, the effect of the trapped gas saturations on the gas relative permeability was studied theoretically.

Experimental Method – Foam Flow Tests

Foam flow tests were carried out in a borosilicate-glass micromodel. The micromodel was etched with an irregular hexagonal pattern that formed a model porous medium, with a Gaussian distribution of pore diameters (mean = 60 µm) and throat widths (mean = 13 µm) (Figure 1). The pattern had a total width of 800 µm (10/11 pores) and an overall length of 60 mm (849 pores), with a channel depth of 5 µm. The permeability of the micromodel was determined experimentally and found to be 0.72 Darcy.

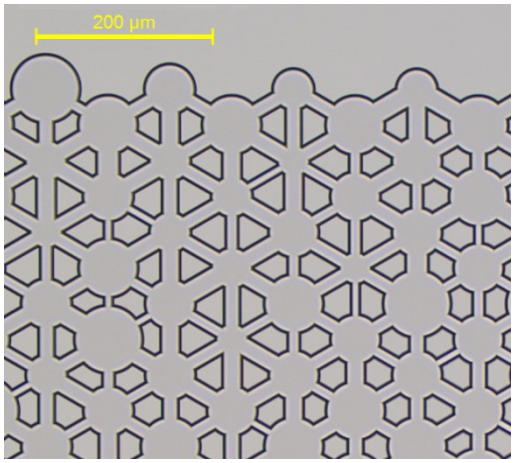

Figure 1 *Photograph of a section of the micromodel, showing the distribution of pore diameters and pore throat widths.*

The chip was viewed using an inverted microscope (Leica DMi8) in Transmitted Light mode, with a X10 objective that allowed for the whole width of the porous channel to be observed. Images of the chip, and the foam flow through the pores, were recorded using a high speed video camera (Photron) connected to the microscope. The video images had a resolution of 1280 x 720 pixels and a typical acquisition rate of 125 frames per second was used.

The foam was generated by coinjecting surfactant solution and nitrogen gas into the micromodel through a frit with 10 µm pores. The surfactant used was a Sodium C14-16 Olefin Sulfonate (AOS) (Bioterge AS-40K) and the solution contained 0.5 wt% total active surfactant with 3 wt% NaCl in demineralized water. The surfactant solution was injected using a syringe pump fitted with a 20 ml stainless steel syringe, which gave a minimum achievable flow rate of 0.25 µL/min (equivalent to a superficial velocity of 1.04×10^{-3} m.s^{-1}). The gas injection was controlled using a mass flow controller with full scale of 0.7 ml/min. The pressure in the system was monitored using two absolute pressure transducers (60 bar full-scale, ±0.04% FS). Once a steady state foam flow was achieved in the chip, the flow behaviour was recorded using the high speed video camera.

The video images were processed and binarised using the ImageJ software package (Rasband, 2016). The trapped gas in the system could then be measured using two different techniques. Firstly, a composite image of consecutive video frames could be generated in ImageJ (Figure 2). The regions of flow could then be identified, where the sequential images of the moving lamellae overlaid to fill the pores with black (see the solid black pore/throat domains in Figure 2). The regions of trapped gas, where the lamellae are stationary, remained white, and a simple image analysis then allowed for the quantification of the trapped gas i.e. the white areas. We could then define a ***trapped area fraction***. This trapped area is calculated as a fraction of the total pore area, so makes a direct measurement of the trapped gas saturation, S_{gt}, within the micromodel [-]. The trapped gas saturation is defined as:

$$S_{gt} = f_{gt} . S_g \ , \tag{1}$$

where f_{gt} is the trapped gas fraction [-] and S_g is the total gas saturation [-].

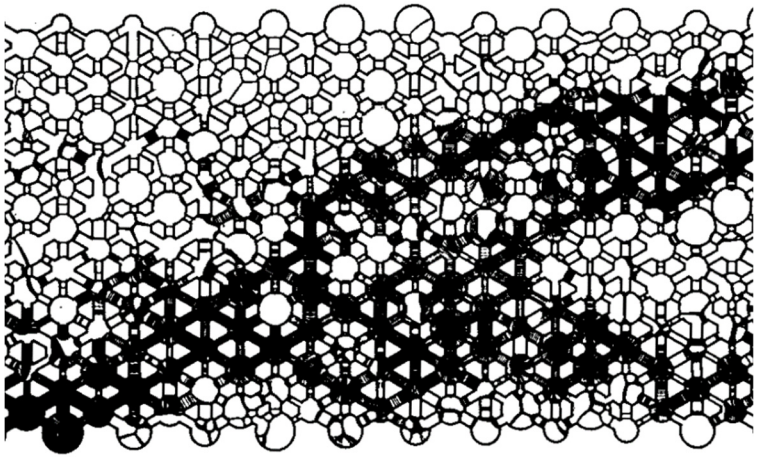

Figure 2 *Composite image of 40 consecutive, binarised video frames. Regions of flow, where the lamellae have moved, show as black, and regions of trapped gas remain white..*

Secondly, the individual bubbles were tracked and their velocities calculated. Bubbles with a velocity beneath a specific threshold were considered trapped. The threshold was set at a finite value (rather than 0) to avoid counting any bubbles that may have been oscillating in position while still remaining trapped in a pore, and also to filter out any small artificial velocities that may have been created during the image processing. The number of trapped bubbles was then described as a fraction of the total number of bubbles, giving a ***trapped bubble fraction***. This gives us a direct measurement of the trapped gas fraction, f_{gt}, within the micromodel.

Using these two measurement techniques, the amount of gas trapped within the micromodel could then be measured as a function of position, flow velocity and foam quality.

Experimental Method – Trapped Gas Model

The theory of foam flooding predicts that the gas relative permeability decreases as certain pores are blocked by trapped gas (Kovscek and Radke, 1994). The relative permeability can capture the effect of the trapped gas via equation 2 below (Falls *et al*. 1989):

$$k_{rg}^{foam} = \frac{k_{rg}(S_g)}{(u_l+u_g)}, \tag{2}$$

where u_l and u_g are the Darcy velocity [m.s^{-1}] and $k_{rg}(S_g)$ is the relative gas permeability [-]. $k_{rg}(S_g)$ is a function of the gas saturation S_g, and has a value derived from the Brooks Corey permeability model for two phases, i.e.

$$k_{rg}(S_g, S_{gt}) = k_{rg}^0 \left(\frac{S_g - S_{gt}}{1 - S_{wc} - S_{gt}}\right)^{n_g}, \tag{3}$$

where the $k_{rg}{}^0$ is the endpoint relative permeability of gas [m^2], S_{wc} is the connate water saturation [-], S_{gt} is the connate or trapped gas saturation [-] and n_g is the gas correlation exponent for the Brooks Corey equation [-].

We know that k_{rg} is function of S_{gt} because, in our experiments, we observed that S_{gt} varied with flow rate and foam quality. The gas saturation, S_g, was measured directly by image processing in the microfluidic experiments. The connate, or residual, water saturation, S_{wc}, was measured in a drainage experiment during which the microchip was first saturated in water and then flooded with gas, and was found to have a value S_{wc} = 0.05 [-]. The saturation of trapped gas S_{gt} can be derived from the fraction

of trapped gas f_{gt} measured in the experiment (eqn. 1). The fraction f_{gt} is measured for different Darcy velocities $u_t=u_l+u_g$ and fractional flows.

The micromodel has a permeability of 719 mD, a value similar to that of the Bentheimer sandstone (773mD) previously tested by Kapetas *et al*. (2015). The Corey parameters for the Bentheimer sandstone were found to be n_g = 0.7 and n_w = 2.86, and these values were used in the current model. The end point of the gas permeability is 0.59 for the Bentheimer sandstone (Kapetas *et al* 2015). The gas relative permeability k_{rg} can then be calculated from equations 1 and 2, using a visual, experimental measurement of the trapped fraction.

The gas relative permeability can also be derived from the experimental pressure measurements across the micromodel using equations 4 and 5.

$$\mu_{foam} = \frac{k|\nabla P|}{u_g+u_l} \quad , \tag{4}$$

where μ_{foam} is the apparent viscosity of the foam [Pa.s], k is the permeability of the porous media [m^2] and ∇P is the pressure gradient [Pa.m^{-1}]. The gas relative permeability k_{rg} can then be calculated using the Darcy law, the definition of the gas fractional flow $f_g=u_g/(u_g+u_l)$, and the gas viscosity μ_g [Pa.s], as expressed in equation 5:

$$k_{rg}(\mu_{foam}) = \frac{f_g \mu_g}{\mu_{foam}} \tag{5}$$

The gas relative permeability is calculated from the experimental measurement of the trapped gas (equations 3) and from the pressure drop (equation 5). If the Brooks Corey model is correct for the 2D micromodel, then equations 3 and 5 should give the same results.

Results and Discussion - Experiments

Initial Flow Behaviour

The initial foam flow through the micromodel showed piston-like flow behaviour, with a sharp flow front (Figure 3). The individual bubbles moved in a stop-start fashion, but this intermittency did not result in any fingering in the flow profile. As the foam front advanced further, some of the bubbles remained trapped in the pores, giving an immediate value of trapped gas within the micromodel. This value was very low however (< 5%) - in the case shown in Figure 3, only 6 bubbles became trapped by the time the foam flow reached the end of the 'observation' frame. It is only when the foam has had time to 'coarsen', where gas diffuses from smaller to larger bubbles (causing the smaller bubbles to disappear), that bubble trapping becomes more significant. The coarsening process can take up to 5 minutes in the current micromodel (Jones *et al*. 2017), so trapped gas measurements were therefore made after the flow was well established and steady state conditions were observed.

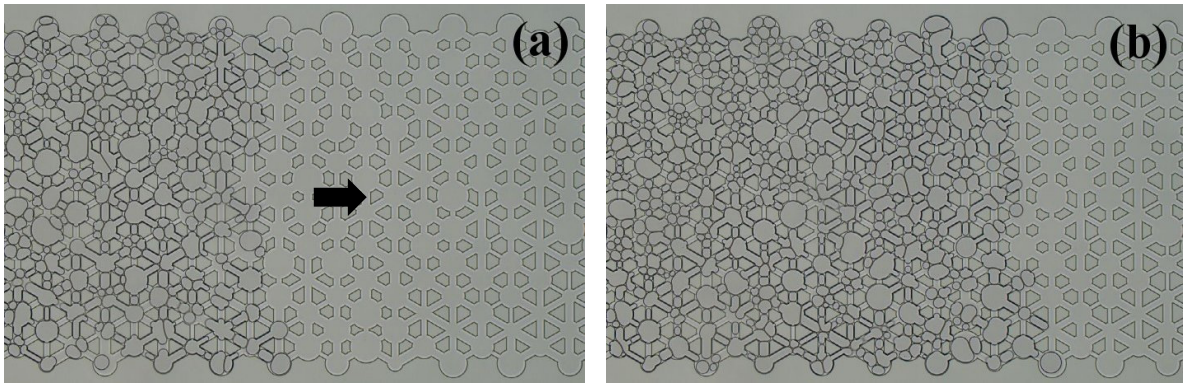

Figure 3 *Plug flow of foam through an initially water saturated micromodel. The foam front is seen at a) t = 1 sec, b) t = 8.3 sec.*

Variation in Trapped Gas with Position in Micromodel

The fraction of trapped gas in the micromodel, f_{gt}, was measured using the trapped bubble-fraction technique, was analysed as a function of position in the micromodel (Figure 4). The position was measured in the flow direction, along the longitudinal axis of the chip with x = 0 at the inlet. The measurements were carried out with a superficial velocity, u, of 0.14 m.s^{-1} and a foam quality, f_q, of 0.3. As can be seen there is very little variation in trapped gas fraction with position in the micromodel and there is no obvious entrance effect observed, as might be expected from the work in corefloods: Eftekhari *et al*. (2015) observed elevated water saturations near the inlet of their core, and Ettinger and Radke (1992) found that both the foam texture and the pressure profile varied near the core inlet, where foam generation mechanisms dominate. It is suggested that any entrance effect is very short in the current geometry, and at the high velocities considered, and is thus not observable in the current experiments.

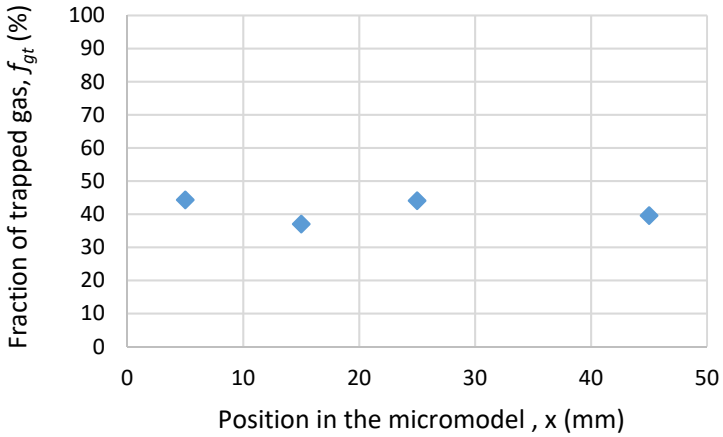

Figure 4 *Trapped gas fraction as a function of position in the micromodel. Positions are defined with respect to the inlet of the micromodel. The measurements were carried out with a foam quality of 0.3 and a superficial velocity of 0.14 m.s^{-1}.*

Variation in Trapped Gas with Total Flow Velocity

Trapped gas fractions were measured, using the trapped bubble fraction technique, for a range of flow velocities (Figure 5) and with foam qualities in the range 0.94 to 0.98. It was found that there was a very strong dependence of the trapped gas fraction on flow velocity, with higher velocities giving reduced values of trapped gas.

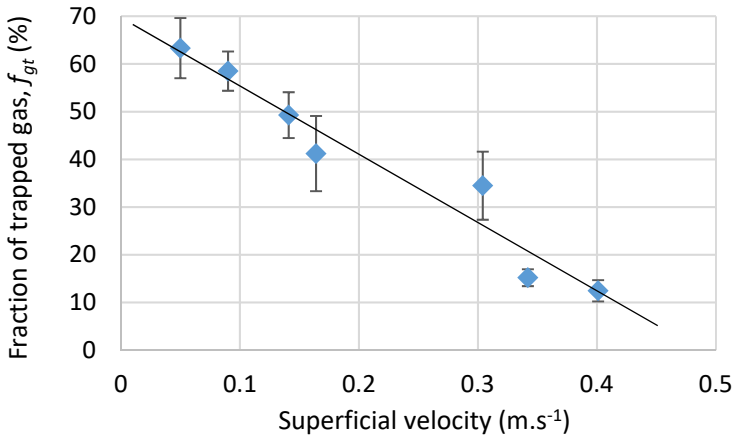

Figure 5 *Trapped gas fraction as a function of the flow rate in the micromodel. Foam quality varies from 0.94 for the lowest flow rate to 0.98 for the highest flowrate. The error bars indicate the range of values obtained with small variations in the velocity thresholding.*

It was also noted that this relationship between trapped gas fraction and velocity was strongly linked to the foam structure within the micromodel. At the lower flow rates, the residence time of the bubbles within the pores was higher, which allowed more time for coarsening. This resulted in a large proportion of the bubbles coarsening to the size of the pores (Figure 6a and Table 1). In general, once a bubble coarsens to the same size as a pore, the surrounding lamellae are found in very stable, low-energy configurations in the pore throats (Nonnekes *et al*, 2016). The energy then required to move the lamellae out of the pore throats becomes significant and only an increase in the driving pressure (Nonnekes *et al*, 2016; Jones *et al*, 2017) or lamella breakage will remobilise these pore-size bubbles. This results in a greater probability of bubbles becoming trapped long term at lower flow-rates, thus giving a higher trapped gas fraction.

At higher velocities, the average bubble size was much smaller than the average pore size (Figure 6b and Table 1) and the foam flow behaviour was more similar to a Newtonian fluid. There was less time for coarsening to occur as the residence time of bubbles at a fixed location was greatly reduced and there were continuous changes in nearest neighbours (thus disrupting the diffusion necessary for coarsening). The amount of trapped gas was therefore greatly reduced.

This result appears to be in direct contradiction to that of Tang and Kovscek (2006), who found that higher gas velocities produced larger bubbles in the effluent. However, they also linked the larger bubble size to a reduction in trapped gas. So both in the work of Tang and Kovscek and in the current study it was found that higher velocities resulted in lower quantities of trapped gas.

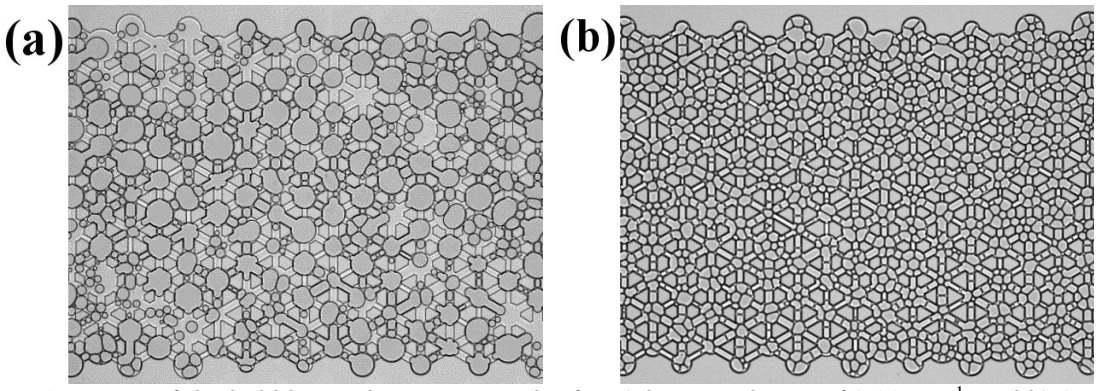

Figure 6 *Images of the bubbles in the porous media for a) linear velocity of 0.09* m.s^{-1} *and b) 0.4* m.s^{-1}*. There is a strong dependence of foam structure on the flow velocity.*

Table 1 *Average bubble size and polydispersity for the two foams shown in Figure 6. The average pore diameter is 60µm, equivalent to an area of 2827 µm².*

Linear Velocity ($m.s^{-1}$)	Number of Bubbles in Frame	Average Bubble Size (μm^2)	Standard Deviation (μm^2)	Polydispersity Index = St.Dev./Average
0.09	510	660	882	1.34
0.4	2566	265	181	0.68

Shear Thinning Behaviour

The shear thinning behaviour of the foam in the micromodel was determined by measuring the pressure drop across the microfluidic chip once steady state was achieved. The apparent viscosity of the foam, $\mu_{foam,app}$, could then be calculated using Darcy's law:

$$\boldsymbol{\mu_{foam,app}} = \frac{\boldsymbol{k\nabla P}}{(\boldsymbol{u_l}+\boldsymbol{u_g})}, \tag{6}$$

where ∇P is the pressure gradient across the micromodel [$Pa.m^{-1}$], u_l and u_g are the liquid and gas superficial velocities respectively [$m\text{-}s^{-1}$], and k is the permeability of the micromodel (0.72 Darcy).

The apparent viscosity was found to vary with the injection flow rate as shown in **Error! Reference source not found.Error! Reference source not found.**, following a typical shear-thinning power-law curve with an exponent of -0.877 (shear thinning curves in Bentheimer rock cores have been found to have exponents in the range -0.5 to -1.0, depending on foam quality: *unpubl. results*). It is noted that the calculated viscosities have very low values, compared to typical foam measurements, but this is linked to the high velocities (~0.5 $m.s^{-1}$) used in this test which are significantly higher than those found in typical core flood experiments (~10^{-5} $m.s^{-1}$).

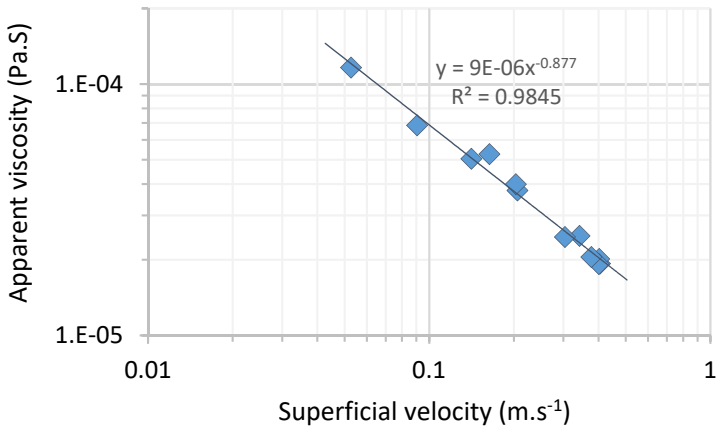

Figure 7 *Measured apparent viscosity of the foam as a function of the velocity.*

It is suggested that one of the reasons for the strong shear thinning response of the foam flow in a porous media is the variation in the quantity of trapped gas with velocity (Figure 5). The higher the quantity of trapped gas, the fewer the number of available flow paths within the medium. This results in a higher resultant pressure gradient, which gives a higher value of measured apparent viscosity. Considering how the apparent viscosity varies with the quantity of trapped gas in the micromodel (Figure 8), it can be seen that there is a strong correlation between the two quantities.

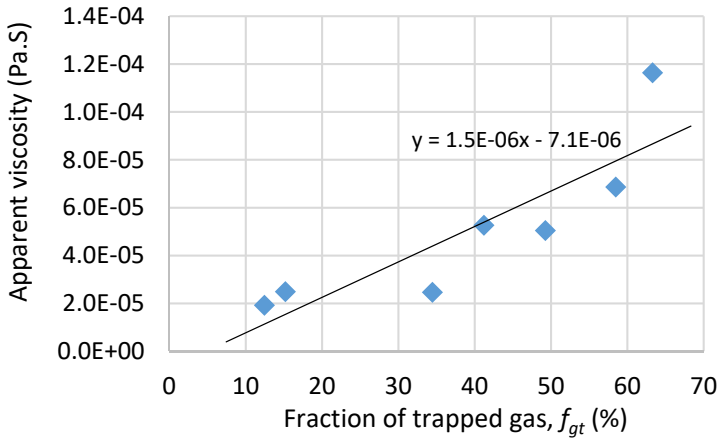

Figure 8 *Variation in measured apparent viscosity with the trapped gas in the micromodel.*

Comparison of Trapped Gas Measurement Techniques

The quantity of trapped gas in the micromodel was determined using the two measurement techniques: firstly, the trapped area fraction (giving S_{gt}) calculated via image analysis, and secondly the trapped bubble fraction (giving f_{gt}) calculated via consideration of the bubbles' velocities, over a range of different velocities. In order to make a good comparison, the values of f_{gt} for the trapped bubble technique were converted to saturations using equation 1 and estimates of S_w (determined from the images of the foam). A comparison of the resultant trapped gas saturations for the two techniques are shown in Figure 9.

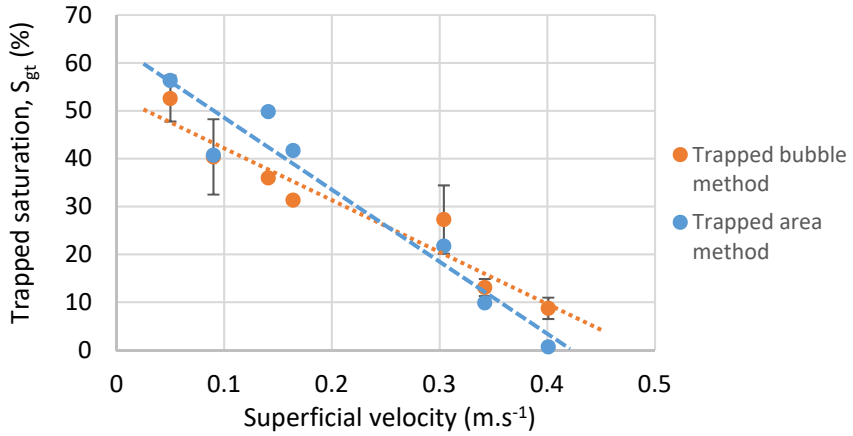

Figure 9 *Trapped gas saturation, measured using the trapped area and the trapped bubble techniques, plotted as a function of the superficial velocity. The error bars in the trapped bubble fraction measurements indicate the range of values obtained with small variations in the velocity thresholding.*

It was found that there was good agreement between the two measurement techniques, although there is a slight difference in the gradients of the resultant trend lines. It should be noted, however, that there are errors inherent with both of the techniques, which would account for the scatter in the data. Considering the trapped area measurement, the calculations from the composite image (Figure 2) assume that all flowing paths are completely filled by the superimposed images of lamellae, when in fact there are gaps. This would then result in an overestimation of the trapped gas saturation. Considering the trapped bubble fraction measurement, there are difficulties in setting an appropriate velocity threshold. If the velocity threshold is set too high, the trapped gas fraction will be overestimated by slow moving bubbles also being counted as trapped. And if the velocity threshold is too low, bubbles that are trapped, but oscillating in place (with a resultant significant velocity), will not be counted as trapped. The error bars in Figure 9 give an indication of the range of different values that can be obtained

with small variation in the velocity thresholding. In both cases, errors could also be introduced into the measurements of the trapped gas due to the effect of fluctuating flow paths (Kil *et al*., 2009).

Variation in Trapped Gas with Foam Quality

The variation of trapped gas fraction with injected foam quality, at a constant superficial velocity of 0.083 m.s^{-1} (equivalent to a flow rate of 20 µL/min), is shown in Figure 10. As the foam quality increases, there is a general trend of decreasing trapped gas, as seen by Tang and Kovscek (2006), although the effect is less strong than that observed with changing velocity.

This effect can again be partly attributed to the foam structure within the micromodel. The experiments showed a general trend of larger bubbles for lower foam qualities and more finely textured bubbles for higher foam qualities (Figure 11). As discussed above, larger bubbles are more likely to occupy the pores and form very stable configurations within the porous network. They therefore have a higher probability of becoming trapped.

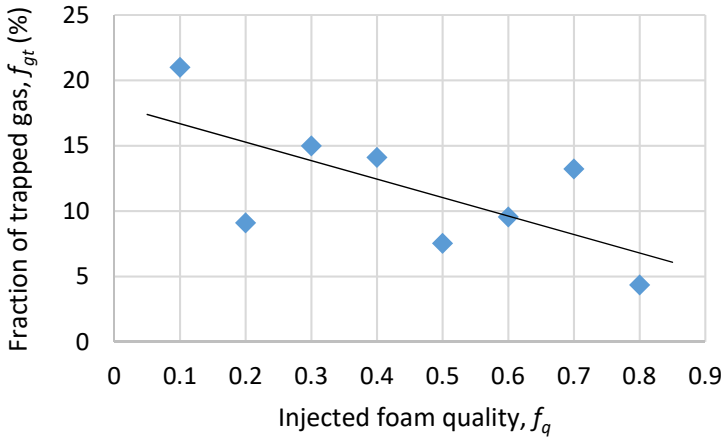

Figure 10 *Trapped gas fraction as a function of the foam quality, for injected foam qualities in the range 0.1 to 0.9, and with a superficial velocity of 0.083 m-s^{-1}.*

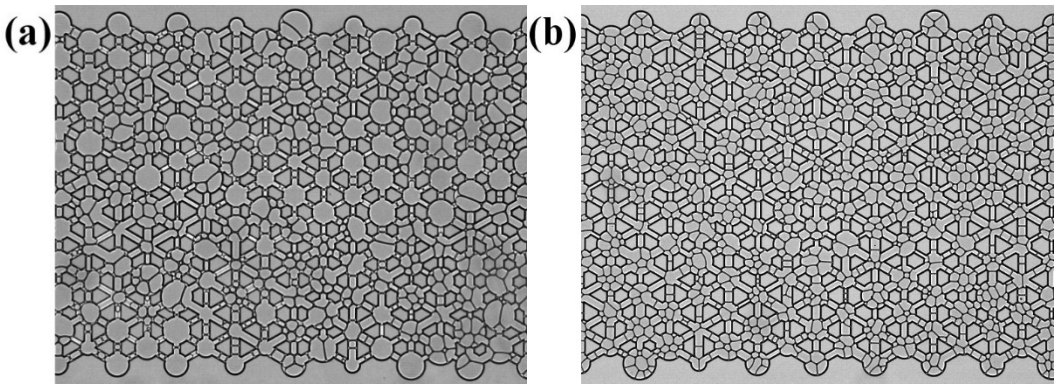

Figure 11 *Images of the bubbles in the porous media for a) foam quality of 0.3 and b) 0.85. There is a variation in the foam structure with the foam quality, with the drier foam showing a finer texture.*

Results and Discussion – Trapped Gas Model

Effect of the Trapped Gas on Relative Permeability

The gas relative permeability k_{rg} was calculated in two different ways: 1) based on the trapped gas saturation S_{gt} measurements, from eqn. 3; and 2) from the apparent viscosity of the foam μ_{foam}, from eqn. 5. The data used for the comparison was from the microfluidic experiments, with superficial velocities varying from 0.05 to 0.4 m.s^{-1} (see Figure 9). As can be seen in Figure 12, the results showed

a linear trend of $k_{gr}(S_{gt})$ with relation to $k_{rg}(\mu_{foam})$, which would indicate that trapped gas S_{gt} is correlated with μ_{foam}.

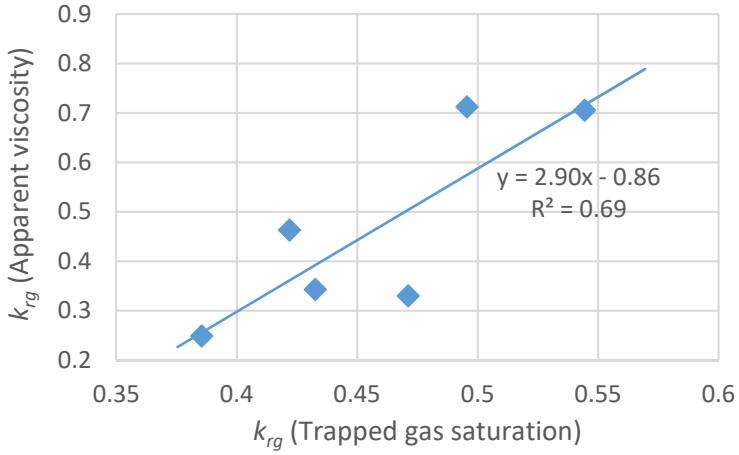

Figure 12 *Gas relative permeability k_{rg} calculated from the foam apparent viscosity μ_{foam}, (equation 5) plotted as function of k_{rg} calculated from the trapped gas S_{gt}, (equation 3).*

However, the data is very scattered, and there are several factors that could have caused this. Firstly, the measurements of S_{gt} were carried out on only a small section of the micromodel, limited by the field of view of the microscope (~ 1mm), as compared to the apparent viscosity measurement which is based on the pressure drop over the full length of the micromodel (6 cm). Thus localized S_{gt} measurements are compared with bulk μ_{foam} measurements, and there is an associated greater degree of scatter in the localized measurements. Secondly, the Corey parameters and end-point relative permeability used in the calculations (eqn. 3) were taken from measurements of Bentheimer sandstone with a similar permeability to the micromodel (Kapetas *et al.*, 2015). However, there are structural differences between the micromodel and the sandstone – the micromodel is a 2-D system, with smooth glass walls and a very high porosity (~ 0.58,) whereas the Bentheimer is a 3D system of irregular grains and lower porosity (~ 0.23) – and these differences may alter the Corey parameters and end-point relative permeabilities. It is suggested that future work should involve measurement of the actual Corey parameters for the micromodel, to improve the accuracy of the model.

Also, it is noted that the slope of the trend in Figure 12 should be 1 if both equations 3 and 5 accurately describe k_{rg}. However, the slope in the current work is approximately 3. It is suggested that this discrepancy is again partly due to the localized/bulk measurement and Corey parameters discussed above. There is also the possibility that there is a constant is missing or inaccurate in equations 3 or/and 5.

Conclusions

Foam flow tests have been carried out in a 2D micromodel to investigate the trapped gas behavior within a porous media. Two different techniques were used to determine the fraction of trapped gas in the micromodel : firstly, a trapped bubble technique, based on velocity thresholding of the foam flow, and secondly, a trapped area technique, based on image analysis. The two techniques were in good agreement, and the following observations have been made:

- There are errors inherent with the two trapped gas measurement techniques, both in the image analysis and the velocity thresholding. However, these errors are in general small, and both of the trapped gas measurement techniques are capable of showing the foam response to changing conditions. It is suggested that either technique would be suitable for future tests, although individual experimental set-ups may bias towards a particular technique.

- It is important to note that the two techniques measure slightly different quantities. The trapped area technique makes a direct measurement of the trapped gas saturation, S_{gt}, and the trapped bubble technique measures the trapped gas fraction, f_{gt} (which can be used to calculate the saturation if the gas saturation, S_g, is known).

- If the foam quality and flow velocity were kept constant, there was no significant difference in trapped gas fraction regardless of the position in the micromodel. There was no observable entrance effect at the flow velocities tested.

- Considering the flow velocity, there was a strong response of the trapped gas to variations in the foam velocity. The trapped gas fraction dropped from 59% to 11% as the velocity increased from 0.05 to 0.4 $m.s^{-1}$. Increasing the total velocity resulted in a reduction of the trapped gas fraction, and this could be linked to the changing foam structure observed at the different flow velocities. Higher flow rates produced finer textured foams that were less likely to block individual pores. At lower flow rates, there was a higher probability of bubbles coarsening to the size of the containing pore; a very stable configuration that would greatly increase the chance of the bubble becoming trapped long term.

- The foam flow also showed strong shear thinning behavior, consistent with behavior previously observed in core-flood studies (Prud'homme, 1995). There is a strong correlation between the shear thinning behavior and the trapped gas within the system.

- Changing the foam quality also produced a response in the level of trapped gas, with drier foams giving lower trapped gas fractions. As with the velocity response, there was again a correlation between the flow behavior and the structure of the foam. Drier foams had a slightly smaller bubble size, which meant that they had a smaller probability of forming the very stable configurations that can block pores.

The trapped gas model was used to calculate the effect of the trapped gas on the gas relative permeability, using both the trapped gas saturation S_{gt} measurements (eqn. 3) and the apparent viscosity of the foam μ_{foam} (eqn. 5), and the following observation were made:

- A linear trend was observed in the plot of $k_{gr}(S_{gt})$ against $k_{rg}(\mu_{foam})$, which would indicate that trapped gas S_{gt} is correlated with μ_{foam}. This would suggest that the apparent viscosity of the foam is mainly due to the trapped gas.

- There was a large degree of scatter in the model data, This could be partly attributed to the fact that the trapped gas saturations, S_{gt} , measurements were highly localized and the apparent viscosity measurements were based on the pressure drop over the whole micromodel i.e. averaged over any localized variations in the trapped gas saturation.

- The Corey parameters and end-point relative permeability used in the model were taken from data for Bentheimer sandstone with a similar permeability to the micromodel. However, there are structural differences between the micromodel and the sandstone, and it is suggested that future work should involve measurement of the actual Corey parameters for the micromodel, to improve the accuracy of the model.

Acknowledgements

We would like to acknowledge the financial support from Shell Global Solution International, and the technical support from Michiel Slob. We thank Dr. Evren Unsal for her careful review of the manuscript and useful comments.

References

Eftekhari, A.A. Krastev, R.and Farajzadeh, R. [2015] Foam stabilized by fly ash nanoparticles for Enhancing Oil Recovery. Ind. Eng. Chem. Res. **54**, 12482–12491

Ettinger, R.A. and Radke, C.J. [1992] Influence of texture on steady foam flow in Berea sandstone. SPE Reserv. Eng. 7, 83–90.

Falls, A. H., Musters, J. J. and Ratulowski, J. [1989] The apparent viscosity of foams in homogeneous bead packs. SPE Reservoir Engineering **4**, 155-164.

Friedmann, F., Chen, W. H. and Gauglitz, P. A. [1991] Experimental and simulation study of high-temperature foam displacement in porous media. SPE Reservoir Engineering **6**, 37-45.

Jones, S.A., Getrouw, N. and Vincent-Bonnieu, S. [2017] Foam coarsening: Behaviour and consequences in a model porous medium. 19th European Symposium on Improved Oil Recovery, P033

Kapetas, L. Vincent-Bonnieu, S., Farajzadeh, R., Eftekhari, A.A., Mohd-Shafian, S.R., Kamarul Bahrim, R.Z. and Rossen, W.R. [2015] Effect of permeability on foam-model parameters - An integrated approach from coreflood experiments through to foam diversion calculations. IOR 2015 - 18th European Symposium on Improved Oil Recovery, Dresden.

Kil, R.A., Nguyen, Q.P. and Rossen, W.R. [2011] Determining trapped gas in foam from computed-tomography images. SPE Journal **16**, 24-34.

Kovscek, A.R. and Bertin, H.J. [2003] Foam mobility in heterogeneous porous media - I: Scaling concepts. Transport in Porous Media **52**, 17-35.

Kovscek, A. R., Patzek, T. W. and Radke, C. J. [1994] Mechanistic prediction of foam displacement in multidimensions: A population balance approach. SPE/DOE Improved Oil Recovery Symposium, Tulsa, Oklahoma, SPE-27789-MS.

Lake, L.W., Johns, R.T., Rossen, W.R. and Pope, G.A. [2014] Fundamentals of Enhanced Oil Recovery. Society of Petroleum Engineers.

Ma, K., Liontas, R., Conn, C.A., Hirasaki, G.J. and Biswal, S.L. [2012] Visualization of improved sweep with foam in heterogeneous porous media using microfluidics. Soft Matter **8**, 10669–10675.

Manlowe, D. and Radke, C. [1990] A pore-level investigation of foam / oil interactions in porous media. SPE Reservoir Engineering **5**, 495–502.

Nonnekes, L.E., Cox, S.J. and Rossen, W.R. [2014] Effect of gas diffusion on mobility of foam for enhanced oil recovery. Transport in Porous Media **106**, 669-689.

Nguyen, Q. P., Rossen, W. R., Zitha, P. L. J. and Currie, P. K. [2009] Determination of gas trapping with foam using X-Ray computed tomography and effluent analysis. SPE Journal **14**, 222-236.

Prud'homme, R. K. [1995] Foams: Theory, Measurements, Applications (Vol. 57). CRC Press.

Radke, C. J. and Gillis, J. V. [1990] A dual gas tracer technique for determining trapped gas saturation during steady foam flow in porous media. SPE Annual Technical Conference and Exhibition, New Orleans, Louisiana, SPE-20519-MS.

Rasband, W.S., ImageJ, U. S. National Institutes of Health, Bethesda, Maryland, USA, http://imagej.nih.gov/ij/, 1997-2016.

Schramm, L.L. [1994] Foams: Fundamentals and Applications in the Petroleum Industry (Vol. 242). American Chemical Society.

Tang, G.-Q. and Kovscek, A.R. [2006] Trapped gas fraction during steady-state foam flow. Transport in Porous Media **65**, 287–307.